Met. Mater. Int., Vol. 19, No. 1 (2013), pp. 99~103
doi: 10.1007/s12540-013-1016-3

Simultaneous Synthesis and Consolidation of Nanocrystalline Fe_2Al_5 and Fe_2Al_5 -Al_2O_3 by Pulsed Current Activated Sintering and Their Mechanical Properties

In-Jin Shon[1,*], Kwon-Il Na[1], Jung-Mann Doh[2], Hyun-Kuk Park[1], and Jin-Kook Yoon[2]

[1]Division of Advanced Materials Engineering and the Research Center of Advanced Materials, Engineering College, Chonbuk National University, 561-756, Korea
[2]Interface Control Research Center, Korea Institute of Science and Technology, PO Box 131, Cheongryang, Seoul 130-650, Korea

(received date: 27 December 2011 / accepted date: 23 February 2012)

Nanopowders of Fe, Al and Fe_2O_3 are fabricated by high energy ball milling. Using the pulsed current activated sintering method, the densification of nanocrystalline Fe_2Al_5 and Al_2O_3 reinforced Fe_2Al_5 composites were simultaneously synthesized and consolidated within two minutes from mechanically activated powders. The advantage of this process is that it allows very quick densification to near theoretical density and prohibition of grain growth in nanostuctured materials. Nanocrystalline materials have received much attention as advanced engineering materials with improved physical and mechanical properties. As nanomaterials possess high strength, high hardness, excellent ductility and toughness, undoubtedly, more attention has been paid to the application of nanomaterials. Not only the hardness but also the fracture toughness of the Fe_2Al_5-Al_2O_3 composite was higher than that of monolithic Fe_2Al_5 due to the addition of the hard phase of Al_2O_3 and the crack deflection by Al_2O_3.

Key words: chemical synthesis, composites, nanostructured materials, toughness, powder processing

1. INTRODUCTION

Iron aluminides are of interest for structural applications at elevated temperature in hostile environments. This is because they generally possess excellent oxidation and corrosion resistance, relatively lower density and lower material cost than Ni-based alloys [1-3]. These properties make iron aluminides a promising candidate for use in the aircraft and automotive industries [1]. However, like many intermetallics, use of iron aluminides in industry has been limited due to low fracture toughness. The mechanical property can be improved significantly by reinforcing iron aluminides with hard ceramic particles such as Al_2O_3 [4] and by fabrication of nanostructured composites [5]. Al_2O_3 has a density of 3.98 g/cm^3, a Young's modulus of 380 GPa, excellent oxidation resistance and good high-temperature mechanical properties [6]. Nanocrystalline materials have received much attention as advanced engineering materials with improved physical and mechanical properties. As nanomaterials possess high strength, high hardness, excellent ductility and toughness, undoubtedly, more attention has been paid to the application of nanomaterials [7,8]. Hence, a nanostructure consisting of iron aluminides and Al_2O_3 may have sufficient oxidation resistance and high temperature mechanical properties to be a successful high temperature structural material.

Nanocrystalline powders were recently developed by such thermochemical and thermomechanical processes as the spray conversion process (SCP), co-precipitation and high energy milling [9-11]. However, the grain sizes in sintered materials become much larger in pre-sintered powders due to fast grain growth during conventional sintering. Therefore, even though the initial particle size is less than 100 nm, the grain size increases rapidly up to 2 μm or larger during conventional sintering [12]. Controlling grain growth during sintering is one of the keys to the commercial success of nanostructured materials. Pulsed current activated sintering, which can yield dense materials within 2 min, is effective for controlling grain growth [13,14].

The purpose of this work is to produce dense nanocrystalline Fe_2Al_5 and Fe_2Al_5-Al_2O_3 composites within 2 min from mechanically activated powders using pulsed current activated sintering and to evaluate their mechanical properties, hardness and fracture toughness.

2. EXPERIMENTAL PROCEDURES

Powders of 99.5% Fe (<10 μm, Alfa, Inc), 99% Fe_2O_3 (<5

*Corresponding author: ijshon@chonbuk.ac.kr

μm, Alfa, Inc) and 99% pure Al (-325 mesh, Cerac. Inc.) were used as a starting materials. 2Fe and 5Al, Fe_2O_3 and 7Al powder mixtures were first milled in a high-energy ball mill, a Pulverisette-5 planetary mill, at 250 rpm for 10 hrs. Tungsten carbide balls (8 mm in diameter) were used in a sealed cylindrical stainless steel vial in an argon atmosphere. The weight ratio of ball-to-powder was 30:1. Milling resulted in a significant reduction in grain size.

The grain sizes of the Fe_2Al_5 and Al_2O_3 were calculated by Suryanarayana and Grant Norton's formula [15],

$$B_r\,(B_{crystalline}+B_{strain})\cos\theta = k\lambda / L + \eta\sin\theta, \quad (1)$$

where B_r is the full width at half-maximum (FWHM) of the diffraction peak after instrumental correction; $B_{crystalline}$ and B_{strain} are the FWHM caused by small grain size and internal stress, respectively; k is constant (with a value of 0.9); λ is the wavelength of the X-ray radiation; L and η are the grain size and internal strain, respectively; and θ is the Bragg angle. The parameters B and B_r follow Cauchy's form with the relationship: $B = B_r + B_s$, where B and B_s are the FWHM of the broadened Bragg peaks and the standard sample's Bragg peaks, respectively.

After milling, the mixed powders were placed in a graphite die (outside diameter, 45 mm; inside diameter, 20 mm; height, 40 mm) and then introduced into the pulsed current activated sintering system made by Eltek in South Korea, shown schematically in reference [13,14]. The four major stages in the synthesis are as follows. Stage 1- Evacuation of the system. Stage 2- Application of uniaxial pressure. Stage 3- Heating of sample by pulsed current (on time; 20 μs, off time; 10 μs). Stage 4- Cooling of sample. Temperatures were measured by a pyrometer focused on the surface of the graphite die. The graphite was heated to 1100 °C with a heating rate of about 600 °C/min. The process was carried out in a vacuum of 40 mTorr (5.33 Pa).

The relative densities of the synthesized sample were measured by the Archimedes method. Microstructural information was obtained from product samples that were polished at room temperature. Compositional and micro structural analyses of the products were completed through X-ray diffraction (XRD) and scanning electron microscopy (SEM) with energy dispersive X-ray analysis (EDAX). Vickers hardness was measured by performing indentations at a load of 10 kg_f and a dwell time of 15 s on the sintered samples. Indentations with large enough loads produced median cracks around the indent. The lengths of these cracks permit estimation of the fracture toughness of the materials by means of the expression [16].

$$K_{IC} = 0.203(c/a)^{-3/2}\cdot H_v\cdot a^{1/2}, \quad (2)$$

where c is the trace length of the crack measured from the center of the indentation, a is one half of the average length of the two indent diagonals, and H_v is the hardness.

3. RESULTS AND DISCUSSION

The interactions between 2Fe and 5Al, and between Fe_2O_3 + 7Al i.e.,

$$2Fe + 5Al \rightarrow Fe_2Al_5 \quad (3)$$
$$Fe_2O_3 + 7Al \rightarrow Fe_2Al_5 + Al_2O_3 \quad (4)$$

are thermodynamically feasible.

X-ray diffraction results of high energy ball milled powders are shown in Fig. 1(a) and (b). The reactant powders Fe, Fe_2O_3 and Al were detected in Fig. 1(a) and Fig. 1(b) but the products Fe_2Al_5 and Al_2O_3 were not detected. The above results confirmed that mechanochemical synthesis did not occur during the high energy ball milling. The average grain sizes of Fe, Fe_2O_3 and Al milled for 10 h measured by Suryanarayana and Grant Norton's formula were lower than 50 nm. Figures. 2(a) and (b) show the X-ray diffraction results of the specimins (2Fe + 5Al, and Fe_2O_3 + 7Al) sintered at 1100 °C by the pulsed current activated sintering. The reactant powders of Fe, Fe_2O_3 and Al were not detected in Figs. 2(a) and (b) but the products Fe_2Al_5 and Al_2O_3 were detected. The above results revealed that mechanochemical synthesis occurred

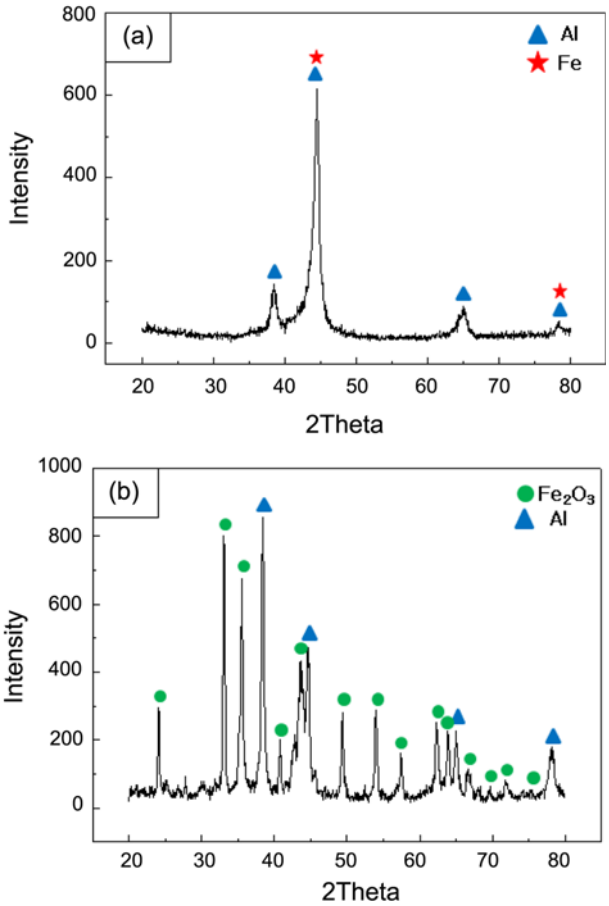

Fig. 1. XRD patterns of mechanically milled powder: (a) 2Fe+5Al system and (b) Fe_2O_3 + 7Al system.

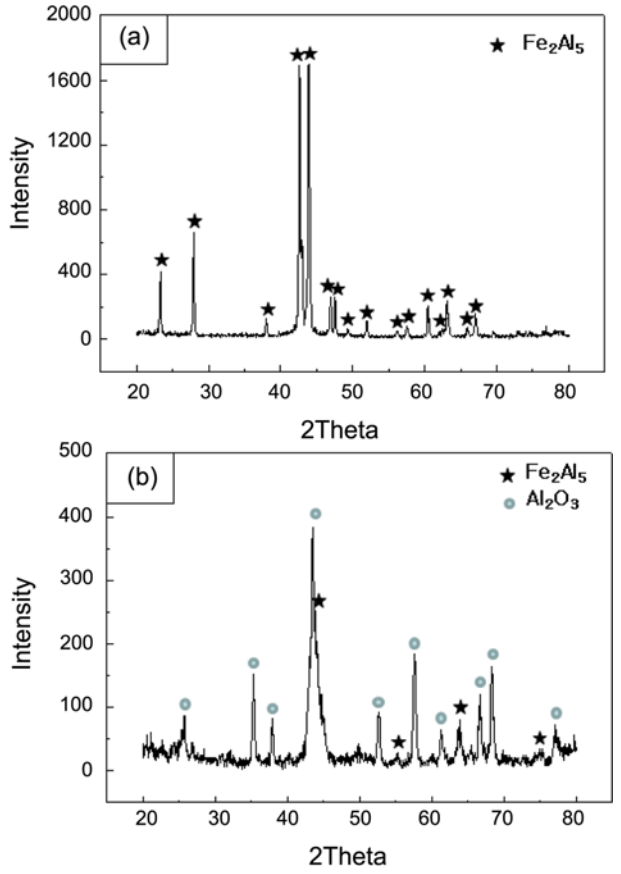

Fig. 2. XRD patterns of specimens sintered at 1100 °C: (a) 2Fe+5Al system and (b) Fe_2O_3 + 7Al system.

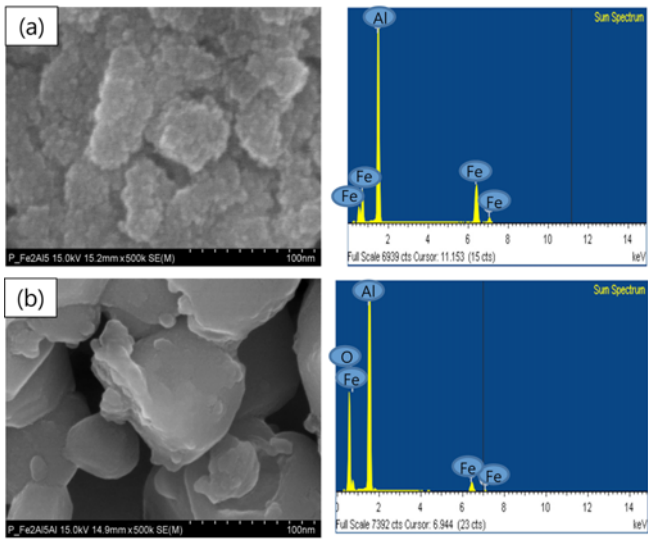

Fig. 3. FE-SEM images and EDS analysis of Fe_2Al_5(a) and Fe_2Al_5-Al_2O_3(b) composites sintered at 1100 °C.

during the heating.

Figures 3(a) and (b) show the FE-SEM image and EDS analysis of Fe_2Al_5 and Fe_2Al_5-Al_2O_3 composites sintered at 1100 °C. The relative densities of the Fe_2Al_5 and Fe_2Al_5-Al_2O_3 composites were about 99% and 97%, respectively. The Fe_2Al_5 and Fe_2Al_5-Al_2O_3 composites consisted of nanocrystallites. Al, Fe, and O peaks were detected in the EDS and heavier contaminants, such as W from a ball, was not detected. Fig. 4 shows a plot of B_r ($B_{crystalline}$+B_{strain}) cosθ versus sinθ of Fe_2Al_5 and Al_2O_3 in the sintered Fe_2Al_5 and Fe_2Al_5-Al_2O_3 composites, respectively. The structure parameters, *i.e.*, the average grain sizes of Fe_2Al_5 sintered from 2Fe+5Al, and Fe_2Al_5 and Al_2O_3 in the Fe_2Al_5-Al_2O_3 composite obtained from the X-ray data by Suryanarayana and Grant Norton's formula were 20, 70 and 30 nm, respectively. The average grain sizes of the sintered Fe_2Al_5 and Fe_2Al_5-Al_2O_3 composite were not significantly larger than the grain sizes of the initial powders, indicating the absence of significant grain growth during sin-

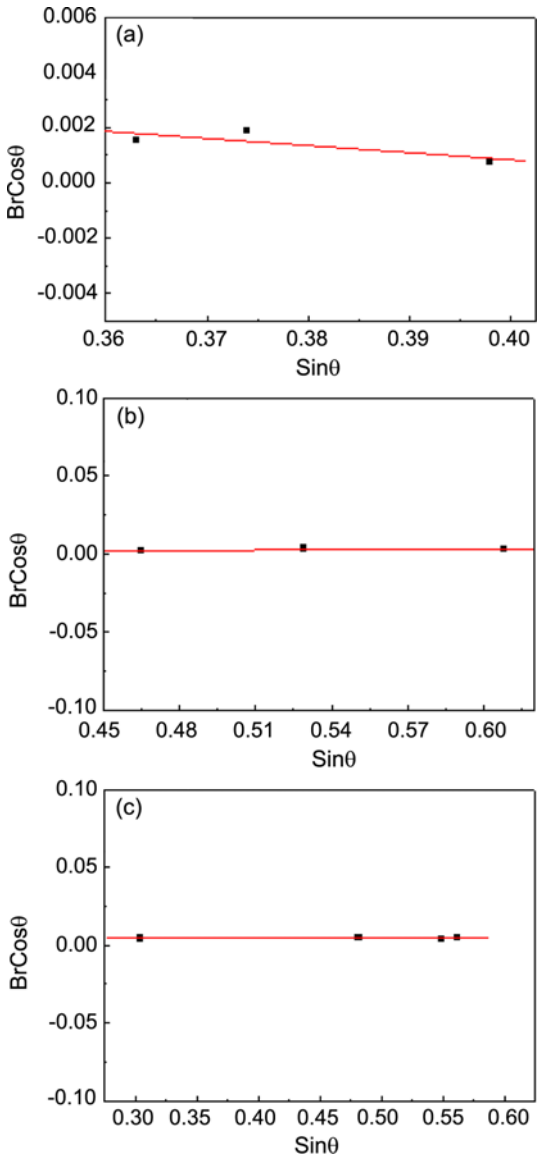

Fig. 4. Plot of B_r ($B_{crystalline}$+B_{strain}) cosθ versus sinθ of Fe_2Al_5(a), Fe_2Al_5(b), and Al_2O_3(c) in sintered Fe_2Al_5 and Fe_2Al_5-Al_2O_3 composites.

tering. We attributed this retention of the grain size to the high heating rate and the relatively short exposure of the powders to the high temperature. The role of current in sintering has been the focus of several attempts to explain the observed enhancement of sintering and the improved characteristics of the products. The role played by the current has been hypothesized to involve a fast heating rate due to Joule heating, the presence of plasma in pores separating powder particles, and the intrinsic contribution of the current to mass transport [17-20].

Vickers hardness measurements were made on polished sections of the Fe_2Al_5 and Fe_2Al_5-Al_2O_3 composite using a 10 kg_f load and 15 s dwell time. The calculated hardness value of the Fe_2Al_5 and Fe_2Al_5-Al_2O_3 composites were 800, and 850 kg/mm^2, respectively. This value represents an average of five measurements.

As in the case of the hardness values, the toughness values were derived from the average of five measurements. The toughness values of the Fe_2Al_5 and Fe_2Al_5-Al_2O_3 composites obtained by the method of calculation were 2.5, and 6 MPa·m$^{1/2}$. Typically, one to three additional cracks were observed to propagate from the indentation corner. Higher magnification views of the indentation median crack in the Fe_2Al_5 and Fe_2Al_5-Al_2O_3 composites are shown in Figs. 5(a) and (b). They show that the crack propagates linearly in the Fe_2Al_5 composite and deflectively (↑) in the Fe_2Al_5-Al_2O_3 composite. Not only the hardness but also the fracture toughness of the Fe_2Al_5-Al_2O_3 composite is higher than that of the monolithic Fe_2Al_5 due to the addition of the hard phase of Al_2O_3 and the crack deflection by Al_2O_3.

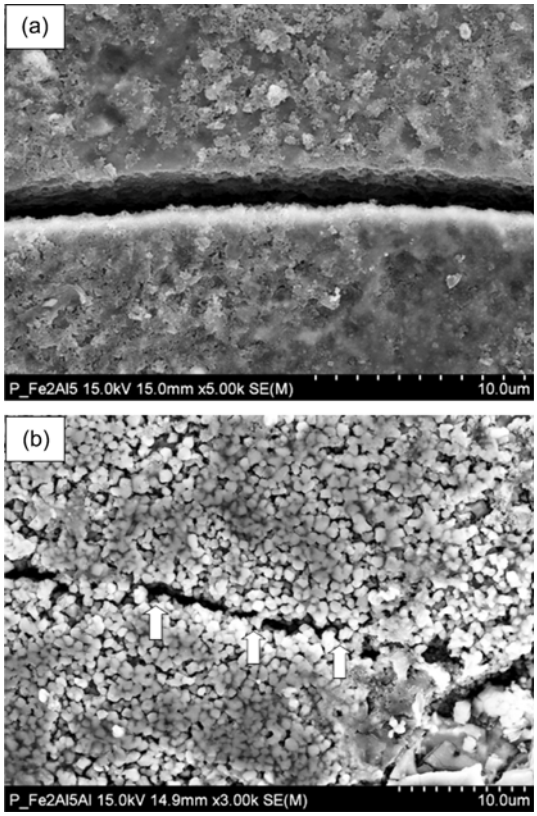

Fig. 5. Median crack propagation in the Fe_2Al_5 composite (a) and the Fe_2Al_5-Al_2O_3 composite (b).

4. CONCLUSIONS

Nanopowders of Fe, Al and Fe_2O_3 were fabricated by high energy ball milling. Using the pulsed current activated sintering method, the densification of nanocystalline Fe_2Al_5 and Al_2O_3 reinforced Fe_2Al_5 composites were created from mechanically activated powders. Complete densification was achieved within 2 min. The relative density of the Fe_2Al_5 and Fe_2Al_5-Al_2O_3 composites were 99 and 97% for an applied pressure of 80 MPa and a pulsed current. The average grain sizes of Fe_2Al_5 sintered from 2Fe+5Al and Fe_2Al_5 and Al_2O_3 in the Fe_2Al_5-Al_2O_3 composites were 20, 70 and 30 nm, respectively. The average hardness and fracture toughness values of the Fe_2Al_5 and Fe_2Al_5-Al_2O_3 composites were 800 kg/mm^2, 850 kg/mm^2, 2.5 MPa·m$^{1/2}$, and 6 MPa·m$^{1/2}$, respectively.

ACKNOWLEDGMENTS

This research was supported by Basic Science Research Program through the National Research Foundation of Korea (NRF) funded by the Ministry of Education, Science and Technology (No, 2012001300) and This work is partially supported by KIST Future Resource Research Program.

REFERENCES

1. C. T. Liu, E. P. George, P. J. Maziasz, and J. H. Schneibel, *Mater. Sci. Eng. A* **258**, 84 (1998).
2. S. C. Deevi and V. K. Sikka, *Intermetallics* **4**, 357 (1996).
3. L. Zheng, X. Peng, and F. Wang, *Corros. Sci.* **53**, 597 (2011).
4. A. Michalski, J. Jaroszewicz, M. Rosinski, and D. Siemiaszko, *Intermetallics* **14**, 603 (2006).
5. L. Z. Zhou, J. T. Guo, G. S. Li, L.Y. Xiong, S. H. Wang, and C. G. Li, *Mater. Des*. **18**, 373 (1997).
6. M. F. Ashby and D. R. H. Jones, *Engineering Materials 1* (International Series on Materials Science and Technology, Vol.34), Pergamon Press, Oxford (1986).
7. M. S. El-Eskandarany, *Alloys. Compd*. **305**, 225 (2000).
8. L. Fu, L. H. Cao, and Y. S. Fan, *Scripta Materialia*. **44**, 1061 (2001).
9. N.-R. Park, I.-Y. Ko, J.-K. Yoon, J.-M. Doh, and I.-J. Shon, *Met. Mater. Int*. **17**, 233 (2011).
10. Z. Fang and J. W. Eason, *Int. J. of Refractory Met. & Hard Mater*. **13**, 297 (1995).
11. A. I. Y. Tok, L. H. Luo, and F. Y. C. Boey, *Mater. Sci. Eng. A*. **383**, 229 (2004-2005).
12. J. Jung and S. Kang, *Scripta Materialia* **56**, 561 (2007).

13. I.-J. Shon, H.-Y. Song, S.-W. Cho, W. Kim, and C.-Y. Suh, *Korean J. Met. Mater.* **50**, 39 (2012).
14. I.-J. Shon, H.-J. Wang, C.-Y. Suh, S.-W. and W. Kim, *Korean. J. Met. Mater.* **49**, 374 (2011).
15. C. Suryanarayana, M. G. Norton, *X-ray Diffraction A Practical Approach*, Plenum Press, p. 213, New York (1998).
16. K. Niihara, R. Morena, and D. P. H. Hasselman, *J. Mater. Sci. Lett*. **1**, 12 (1982).
17. Z. Shen, M. Johnsson, Z. Zhao, and M. Nygren, *J. Am. Ceram. Soc.* **85**, 1921 (2002).
18. J. E. Garay, U. Anselmi-Tamburini, Z. A. Munir, S. C. Glade, and P. Asoka-Kumar, *Appl. Phys. Lett.* **85**, 573 (2004).
19. J. R. Friedman, J. E. Garay, U. Anselmi-Tamburini, and Z. A. Munir, *Intermetallics* **12**, 589 (2004).
20. J. E. Garay, U. Anselmi-Tamburini, and Z. A. Munir, *Acta. Mater.* **51**, 4487 (2003).